Neoplasia 37 (2023) 100877

Contents lists available at ScienceDirect

Neoplasia

journal homepage: www.elsevier.com/locate/neo

Identification and characterization of circular RNAs as novel putative biomarkers to predict anti-PD-1 monotherapy response in metastatic melanoma patients – Knowledge from two independent international studies ☆

Jian-Guo Zhou [a,b,c,d,1,2], Rui Liang [e,1], Hai-Tao Wang [f], Su-Han Jin [g], Wei Hu [a], Benjamin Frey [b,c,d], Rainer Fietkau [c,d], Markus Hecht [h], Hu Ma [a,2,**], Udo S. Gaipl [b,c,d,2,*]

[a] Department of Oncology, The second affiliated Hospital of Zunyi Medical University, Zunyi, China
[b] Translational Radiobiology, Department of Radiation Oncology, Universitätsklinikum Erlangen, Erlangen, Germany
[c] Department of Radiation Oncology, Universitätsklinikum Erlangen, Erlangen, Germany
[d] Comprehensive Cancer Center Erlangen-EMN, Erlangen, Germany
[e] Biomedical Engineering College of Bioengineering, Chongqing University, Chongqing, China
[f] Thoracic Surgery Branch, National Cancer Institute, National Institutes of Health, Bethesda, Maryland, USA
[g] Department of Orthodontic, School of Stomatology, Zunyi Medical University, Zunyi, China
[h] Department of Radiotherapy and Radiation Oncology, Saarland University Medical Center, Homburg, Germany

ARTICLE INFO

Keywords:
circRNAs
Predictor
Advanced melanoma
Survival benefit
Anti-PD-1

ABSTRACT

Melanoma is the most aggressive skin malignancy with high morbidity. Anti-programmed cell death protein 1 (PD-1) monotherapy has been applied in metastatic melanoma. However, still most of the patients do not respond to anti-PD-1 and the availability of the present approved biomarkers therefore is limited. Here we combined the transcriptomic and clinical data of 163 advanced melanoma patients receiving anti-PD-1 from NIH Melanoma Genome Sequencing Project (phs000452, 122 patients) as the training and internal validation cohort, and Melanoma Institute Australia cohort (PRJEB23709, 41 patients) as the external validation cohort, respectively. Circular RNAs (circRNAs) are an evolutionarily conserved novel class of noncoding endogenous RNAs (ncRNAs) found in the eukaryotic transcriptome and were used based on RNAseq data for our analyses. 74,243 circular RNAs (circRNAs) were identified with NCLscan and CIRCexplorer2. Thereof, 70 circRNAs significantly associated with progression-free survival and overall survival. Further, a prognostic circRNAs signature consisting of HSA_CIRCpedia_1497, HSA_CIRCpedia_12559, HSA_CIRCpedia_43640, HSA_CIRCpedia_43070, and HSA_CIRCpedia_21660 could be determined with LASSO regression. This signature was a prognostic factor of overall survival and progression-free survival among the analyzed advanced melanoma patients. The concordance indexes (C-index of $OS_{training}$: 0.61, C-index of $PFS_{training}$: 0.68) also confirmed its credibility and accuracy. First enrichment analysis indicated that immune response and pathways related to tumor immune microenvironment were enriched. In conclusion, we succeeded to construct and validate novel prognostic circRNAs signature for advanced melanoma patients treated with anti-PD-1 immunotherapy.

Abbreviations: PD-1, Programmed Cell Death Protein 1; ICI, Immune checkpoint inhibitor; ncRNA, noncodingendogenous RNA; circRNA, circular RNA; mRNA, messenger RNA; EMBL, European Molecular Biology Laboratory; EBI, European Bioinformatics Institute; PFS, Progression-Free Survival; OS, Overall Survival; C-index, Concordance Index; GO, Gene Ontology; GSEA, Gene Set Enrichment Analysis; LASSO, Least Absolute Shrinkage and Selection Operator; NR, Not Reach; HR, Hazard Ratio; CI, Confidence Interval.

☆ Declaration of Competing Interest: The authors declare no relevant conflict of interest regarding this manuscript.

* Corresponding author at: Department of Radiation Oncology, Universitätsklinikum Erlangen, Friedrich-Alexander-Universität Erlangen-Nürnberg (FAU), Universitätsstraße 27, 91054 Erlangen, Germany.
** Corresponding author at: Intersection of Xinlong And Xinpu Avenue, 563000, Zunyi, China
E-mail addresses: mahuab@163.com (H. Ma), udo.gaipl@uk-erlangen.de (U.S. Gaipl).

[1] JGZ and RL contributed equally as first authors.
[2] JGZ, HM and USG contributed equally as senior authors.

https://doi.org/10.1016/j.neo.2023.100877
Received 12 October 2022; Received in revised form 29 December 2022; Accepted 16 January 2023

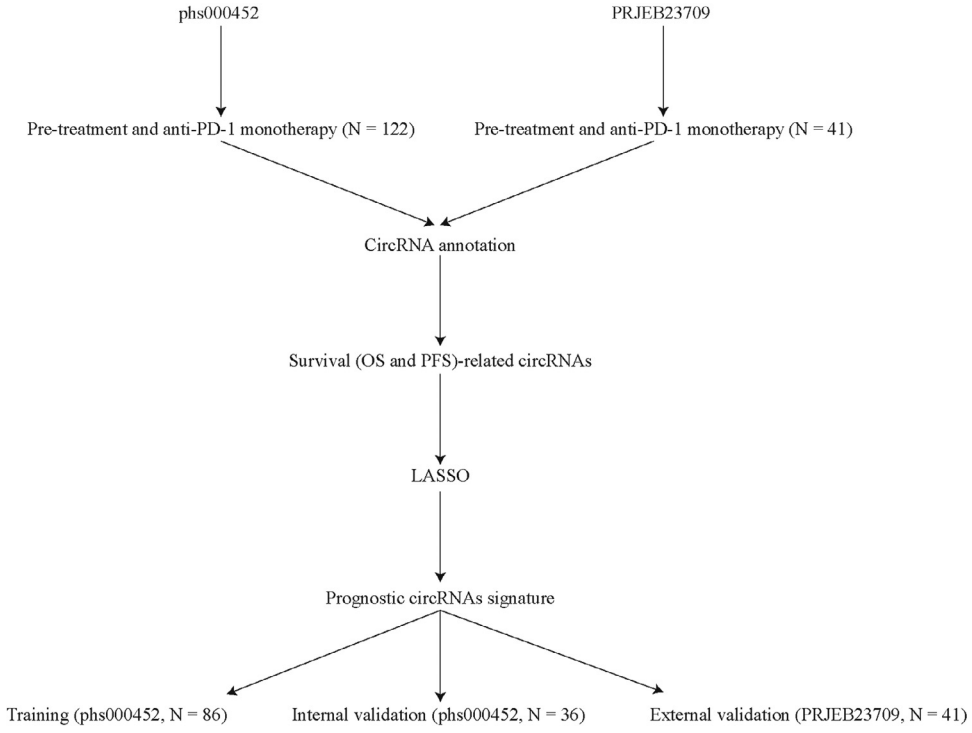

Fig. 1. Flow chart.

Introduction

Immune checkpoint inhibitors (ICIs) have achieved a good extension of survival in some cancer patients in a wide array of cancer types, including metastatic melanoma [1–3], advanced colorectal cancer [4,5], and advanced non-small-cell lung cancer [6,7]. But, still the minority of tumor patients with these entities respond to immune checkpoint inhibitors [8]. Nowadays, many tumor-intrinsic and tumor-extrinsic biomarkers for melanoma response and resistance to ICIs have been proposed [9,10]. However, the clinical response rate did not extensively improve [11]. In general, identification and validation of biomarkers for predicting clinical response and prognosis is needed for patients with metastatic melanoma.

Circular RNAs (circRNAs) are an evolutionarily conserved novel class of noncoding endogenous RNAs (ncRNAs) found in the eukaryotic transcriptome, originally believed to be aberrant RNA splicing by-products with decreased functionality [12]. CircRNAs are unusually stable RNA molecules with cell type- or developmental stage-specific expression patterns [13,14]. Compared to the linear RNA, circRNAs are produced differentially by back-splicing exons or lariat introns from a pre-messenger RNA (mRNA) forming a covalently closed-loop structure missing 3′ poly-(A) tail or 5′ cap, rendering them immune to exonuclease-mediated degradation [15,16]. CircRNAs could be dysregulated in cancer, resulting in distinct circRNA expression profiles in tumor tissues [17,18], which makes it possible to consider circRNAs as biomarkers. To the best of our knowledge, the ability of circRNA-based signatures as novel prognostic biomarkers for melanoma has not yet been comprehensively investigated.

Here, we used phs000452 [19] as the training and internal validation cohorts and PRJEB23709 [20] as the external validation cohort, respectively, to explore the ability of circRNAs to predict the clinical response and prognosis in patients with metastatic melanoma (Fig. 1). We aimed to identify and validate a circRNA-based signature as clinical benefit predictor for advanced melanoma patients treated with anti-PD-1 monotherapy.

Material and methods

Data acquisition

Raw sequencing data of NIH Melanoma Genome Sequencing Project (phs000452 [19]) and Melanoma Institute Australia cohort (PRJEB23709 [20]) were obtained from in dbGaP (accession number phs000452.v.3.p1) and European Molecular Biology Laboratory-European Bioinformatics Institute (EMBL-EBI) [21] (accession number PRJEB23709), respectively. Only pretreatment bulk RNAseq data of metastatic melanoma patients who received anti-PD-1 monotherapy (nivolumab or pembrolizumab) were included in our study.

Alignment

Raw RNA-sequencing reads were aligned to the reference genome (UCSC hg38 with annotations from GRCh38.p13) using STAR [22] (v.2.5.3a), and gene expression was subsequently quantified using *featureCounts* function of *Subread* package [23] (v.2.0.1), as described previously [24].

CircRNA annotation

Since circRNA is less studied than other noncoding RNAs [25], we annotated it with two annotation methods to ensure the accuracy and repeatability of annotation results. NCLscan utilized a stepwise alignment strategy to almost completely eliminate false calls without sacrificing true positives, enabling it outperforms other publicly-available tools [26]. CIRCexplorer2 systematically annotated different types of alternative back-splicing and alternative splicing events in circRNAs [27]. In each dataset, we annotated circRNA with two pipelines (NCLscan and CIRCexplorer2), and then selected the intersection circRNAs to obtain the corresponding data matrix via *initCircRNAprofiler* function of *circRNAprofiler* package [28] (v.1.9.2). The finial circRNA matrix was quantified based on NCLscan.

Table 1
Characteristics of patients in the training and validation cohorts

	Training cohort (phs000452, N=86)	Internal validation cohort (phs000452, N=36)	External validation cohort (PRJEB23709, N=41)
Male	54	17	26
Age (years)			65
Treatment			
Pembrolizumab	48	23	32
Nivolumab	38	13	9
Responses			
Complete response	11	5	4
Partial response	22	10	15
Mixed response	1	1	0
Stable disease	13	3	6
Progressive disease	39	17	16
Survival time (days)			
Progression-free survival	378	332	511
Overall survival	576	559	680
Status			
Alive	43	17	17
Dead	43	19	24

Data are shown as number or average.

Identification of the prognostic circRNAs

All annotated circRNAs of two datasets were intersected to obtain the overlapping circRNAs. Then, we performed survival analysis to determine the relationship between these filtered circRNAs and progression-free survival (PFS) and overall survival (OS). OS was defined as the time between first application of PD-1 blockade and date of death (any cause). For subjects without documentation of death, OS was censored on the last date the subject was known to be alive. PFS was defined as the time between first application of PD-1 blockade and date of documented disease progression. For subjects without documentation of progression, PFS was censored on the last date the subject was known to be without progression. Only these circRNAs with statistical differences ($P < 0.2$) in both PFS and OS were considered as prognostic circRNAs.

Identification of the prognostic circRNAs signature

Patients in phs000452 were randomly divided into 7:3 as the training cohort and the internal validation cohort, respectively. Patients in PRJEB23709 were considered as the external validation cohort. We conducted logistic LASSO regression, a shrinkage technique that can select a more relevant and interpretable set of predictors [29], to establish prognostic circRNAs signature. We used the *glmnet* package (v.2.2.1) to complete the logistic LASSO regression. All circRNAs in the identifiable signature were annotated in CIRCpedia (v.2) [30].

Validation of the prognostic circRNAs signature

After identification of prognostic circRNAs signature, we used the established signature to divide the patients in both the training cohort and validation cohort into high and low-risk groups through a median [31] identified by *survivalROC* package [32], and then analyzed the OS. Moreover, we also analyzed the PFS. Finally, the concordance index (C-index) was calculated by *cindex* function in *pec* package (v. 2021.10.11), as described previously [33].

Functional analysis

To evaluate the potential biological functions of the prognostic circRNAs signature, we conducted Gene Ontology (GO) and gene set enrichment analysis (GSEA) in phs000452, as described previously [34,35].

Quantification of immune microenvironment

Finally, the abundances of diverse immune and stromal components were quantified using the *IOBR* package (v.0.99.9), which is perform comprehensive analysis of tumor microenvironment and signatures for immuno-oncology [36]. We used *xCell* [37] algorithm in *IOBR* package to calculate the scores of infiltrating cells of each sample in phs000452.

Results

Patient characteristics

We included 122 and 41 patients treated with anti-PD-1 immunotherapy from phs000452 and PRJEB23709, respectively, in our present analyses. After random grouping, there were 74 patients in the training cohort and 48 patients in the internal validation cohort. The characteristics of patients are shown in Table 1. Clinical responses were defined as complete response, partial response, mixed response, stable disease, and progressive disease according to Response Evaluation Criteria in Solid Tumors (RECIST, v.1.1) [38]. Patients were classified as mixed responders when achieving unequivocal responses in individual existing lesions but also progression in others or new lesions [19].

Identification of the prognostic circRNAs

Through NCLscan and CIRCexplorer2, we annotated 74,243 circRNAs (Table S1). Then according to the initial survival analysis, we obtained 392 OS related circRNAs and 408 PFS related circRNAs in the phs000452 cohort, 840 OS-related circRNAs and 1423 PFS-related circRNAs in the PRJEB23709 cohort (Table S2). After taking the intersection of the results of the training cohort and training cohorts, we obtained 70 prognostic circRNAs (Fig. S1).

Identification and Validation of the prognostic circRNAs signature

Through the logistic LASSO regression model, we shrank from 70 prognostic circRNAs to five prognostic circRNAs (HSA_CIRCpedia_1497, HSA_CIRCpedia_12559, HSA_CIRCpedia_43640, HSA_CIRCpedia_43070, and HSA_CIRCpedia_21660) (details are shown in Table 2) to fit a prognostic circRNAs signature.

The median of score as optimal cutoff value that could be used for the prognostic circRNAs signature to stratify these patients into the high or low-risk group in the training cohort (Fig. 2A) was -0.107. The 74 patients of the high-risk group (n = 38) had a median OS of 14.2 months (9.96~not reach (NR)) and the low-risk group (n = 36) of NR(31.82~NR). Compared to the high-risk group, thelow risk group significantly exhibited prolonged OS (hazard ratio (HR) = 0.404, 95% confidence interval (CI) = 0.199~0.821, $P = 0.012$, Fig. 2B). All of the 48 patients in the internal validation cohort were segregated into the

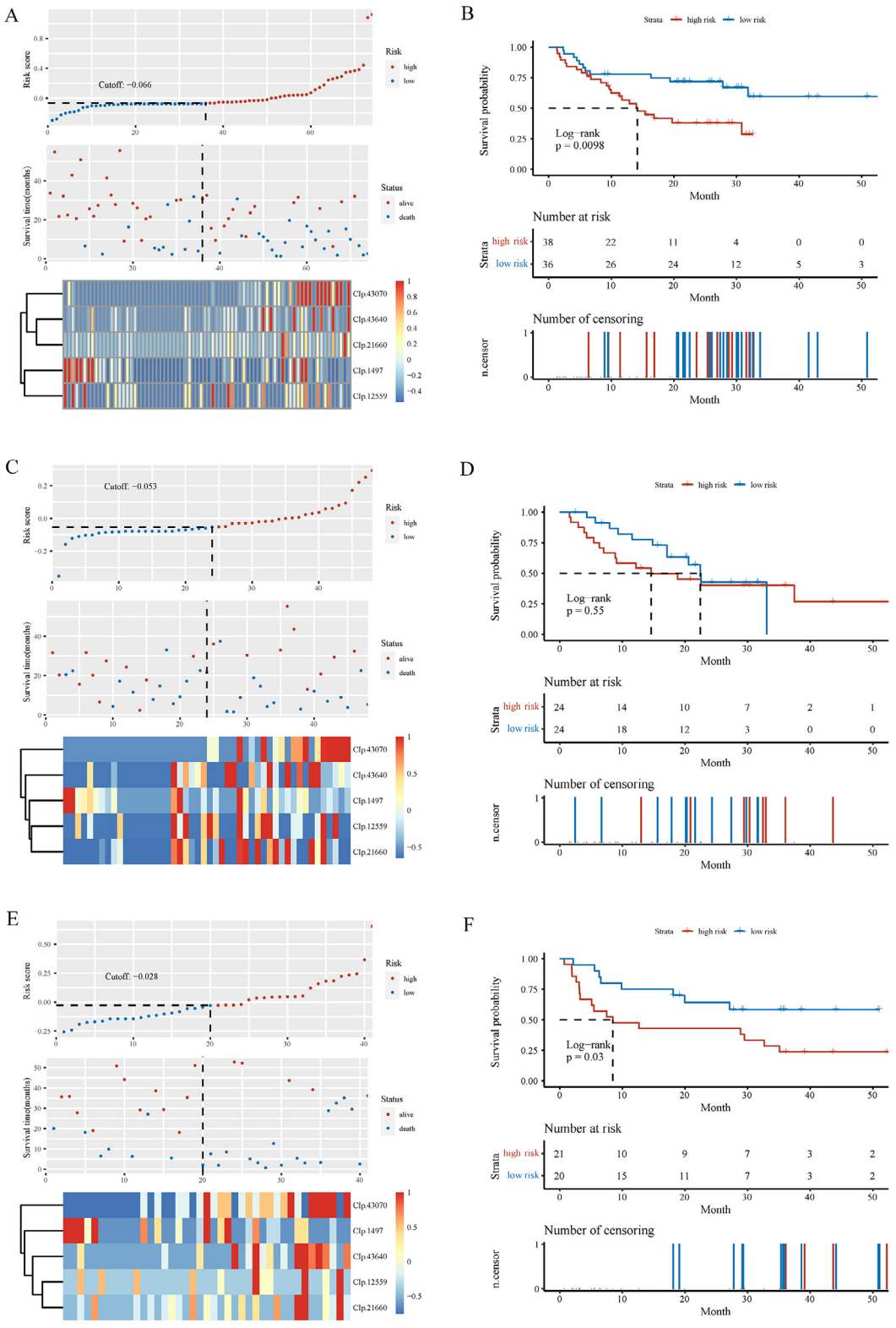

Fig. 2. Characteristics of the prognostic circRNAs signature and Kaplan-Meier estimates for OS in the training and validation cohorts. A. Characteristics of the prognostic signature in the training cohort. top: the risk score of each patient in the training cohort; middle: OS and survival status of patients in the training cohort; bottom: heat map of gene expression profiles of patients in the training cohort. B. OS in the training cohort stratified by the prognostic signature into high and low-risk groups with the *P* value shown. C. Characteristics of the prognostic signature in the internal validation cohort. top: the risk score of each patient in the internal validation cohort; middle: OS and survival status of patients in the internal validation cohort; bottom: heat map of gene expression profiles of patients in the internal validation cohort. D. OS in the internal validation cohort stratified by the prognostic signature into high and low-risk groups with the *P* value shown. E. Characteristics of the prognostic signature in the external validation cohort. top: the risk score of each patient in the external validation cohort; middle: OS and survival status of patients in the external validation cohort; bottom: heat map of gene expression profiles of patients in the external validation cohort. F. OS in the external validation cohort stratified by the prognostic signature into high and low-risk groups with the *P* value shown. The black dotted line represents the prognostic signature cutoff dividing patients into high and low-risk groups, and the *P* value was calculated using the log-rank test.

Table 2
Details of 5 prognostic circRNAs

circID	Gene	Isoform	Location	Strand	Coefficient
HSA_CIRCpedia_1497	*KIF5B*	ENST00000302418.4	chr10:32021287-32019858	-	-0.04814655
HSA_CIRCpedia_12559	*MNAT1*	NM_002431	Chr14:60796217-60818847	+	-0.02206798
HSA_CIRCpedia_43640	*RYK*	ENST00000460933.5	chr3:134195182-134175609	-	0.04626255
HSA_CIRCpedia_43070	*TIMMDC1*	NM_016589	chr3:119500695-119517315	+	0.14014806
HSA_CIRCpedia_21660	*VMP1*	ENST00000262291.8	Chr17:59731421-59773885	+	0.10766172

high-risk group (n = 24) and the low-risk group (n = 24) (Fig. 2C). The low-risk group displayed a median OS of 22.5 month (17.13~NR), and the high-risk group a median OS of 14.6 month (8.84~NR). There was a statistically significant difference between low-risk and high-risk groups (HR = 0.790, 95% CI = 0.362~1.722, $P = 0.553$, Fig. 2D). In the external validation cohort, the median OS was NR (19.96~NR) in low-risk cases (n=20), 8.48 (3.25~NR) months in high-risk cases (n = 21) (Fig. 2E). The low-risk group exhibited significantly longer OS than the high-risk group (HR = 0.401, 95% CI = 0.171~0.941, $P = 0.036$, Fig. 2F). In the training cohort, the prognostic circRNAs signature reached C-index value of 0.683 for OS. In the internal validation cohort, the prognostic circRNAs signature reached C-index value of 0.577 for OS. The external validation cohort was characterized by C-index value of 0.610 for OS.

As for PFS, the low-risk group in the training cohort exhibited significantly better PFS than the high-risk group (HR = 0.404, 95% CI = 0.199~0.821, $P = 0.012$, Fig. 3A&B). The low-risk group in the internal validation cohort exhibited significantly better PFS than the high-risk group with no statistical difference (HR = 0.790, 95% CI = 0.362~1.722, $P = 0.553$, Fig. 3C&D). The high-risk group in the external validation cohort exhibited significantly worse PFS than the low-risk group with no statistical difference (HR = 0.550, 95% CI = 0.291~1.039, $P = 0.066$, Fig. 3E&F). As for PFS, the training, internal validation, and external validation cohorts were characterized by C-index values of 0.683, 0.577, and 0.603, respectively.

Functional analysis

We found that down-regulated genes in phs000452 were enriched in G protein coupled receptor signaling pathway, nervous system process, and various stimuli and senses (Fig. 4A), whereas central nervous system and brain development were activated in the up-regulated genes (Fig. 4B). GSEA indicated some well-known pathways, such as FGFR3 ligand, IFNA signaling, and TRAF6 mediated IRF7 were enriched in the down-regulated genes (Fig. 4C), and IL-37 signaling, KIT signaling, NK cell pathway, and NOTCH signaling were enriched in the up-regulated genes (Fig. 4D).

Quantification of immune microenvironment

We finally compared the abundances of the immune cells between the high- and low-risk groups in phs000452. The abundances of B cells, $CD4^+$ naïve T cells, $CD8^+$ T cells, $\gamma\delta$ T cells, and platelets were lower in the low-risk group than in the high-risk group ($P = 0.034$, 0.007, 0.029, 0.026, and 0.008, respectively, Fig. 5A~E). While the abundance of endothelial cells was higher in the low-risk group than in the high-risk group ($P = 0.045$, Fig. 5F).

Discussion

RNA-sequence-based prognostic signatures could provide good prognostic or diagnostic value for the disease [31,39,40]. Our previous study demonstrated that lncRNAs signature is a novel effective predictor for prognosis in advanced melanoma patients treated with anti-PD-1 monotherapy [24], however, the prognostic role of circRNA in these special population is unknown. Here, we combined two mainstream circRNA annotation methods (NCLscan [26] and CIRCexplorer2 [27]) to annotate up to 74,243 circRNAs, and identified 70 survival related circRNAs after survival analysis of OS and PFS in two different datasets (phs000452 [19] and PRJEB23709 [20]). Then, we identified the prognostic circRNAs signature composed of five prognostic circRNAs (HSA_CIRCpedia_1497, HSA_CIRCpedia_12559, HSA_CIRCpedia_43640, HSA_CIRCpedia_43070, and HSA_CIRCpedia_21660) through LASSO regression in training cohort and validated at independent external cohort. The final functional enrichment analysis also showed that they were related to nervous system process and currently known pathways such as G protein coupled receptor signaling, FGFR3 ligand, IFNA signaling, TRAF6 mediated IRF7, IL-37 signaling, KIT signaling, NK cell pathway, and NOTCH signaling.

Previous studies have confirmed the important role of circRNAs in the occurrence and development of advanced melanoma. For instance circ-GLI1 promotes melanoma metastasis through interacting with p70S6K2 to activate Hedgehog/GLI1 and Wnt/β-catenin pathways and upregulate Cyr61 [41], circ_0020710 drives melanoma progression and immune evasion by regulating the miR-370-3p/CXCL12 axis [42]. To our best knowledge, this study identified the first cirRNA signature to predict survival benefit for advanced melanoma patients treated with immunotherapy. None of these circRNAs have been reported before. Moreover, since we only included the patients treated with anti-PD-1 monotherapy, our reported prognostic circRNAs signature can not only sort out population with different survival benefits, but also serve as biomarkers for immunotherapy.

We grouped all advanced melanoma patients from phs000452 and PRJEB23709 into the high and low-risk groups according to the median of prognostic circRNAs signature. Patients in the high-risk group from both phs000452 and PRJEB23709 shared worse OS, and the C-index indicated that prognostic circRNAs signature we established here was highly efficient in predicting survival benefit of advanced melanoma. Moreover, all patients from phs000452 and PRJEB23709 in the low-risk group shared better PFS. Finally, we enriched the nervous system process and various stimuli and senses, which is related to melanoma. Additionally, some signaling pathways were found to be enriched in our analyses. Previous studies indicated that activation of G protein-coupled estrogen receptor signaling inhibits melanoma and improves response to immune checkpoint blockade [43] and the adhesion G protein coupled receptor, GPR56/ADGRG1, inhibits cell-extracellular matrix signaling to prevent metastatic melanoma growth [44].

A phosphoproteomic platform identified that FGFR3 may be activated via autocrine circuits in melanoma [45], and FGFR3 not only promotes the growth and malignancy of melanoma by influencing EMT [46] but also reactivates MAPK pathway to mediate vemurafenib resistance in melanoma [47]. IFN induces PD-L1 expression depends on p53 [48] and drives clinical response to immune checkpoint blockade therapy in melanoma [49]. IL-37 was up-regulated in melanoma and highly elevated IL-37 in specific lymphocyte populations could serve as a biomarker for melanoma-induced immunosuppression [50]. Activating KIT mutations are rarely found to cause melanomas and may provide an actionable target for therapy [51]. Exosomes derived from natural killer cells exert therapeutic effect in melanoma [52], and later study indicated that STING agonist loaded lipid nanoparticles overcame anti-PD-1 resistance in melanoma lung metastasis via natural killer cell activation [53]. Many studies have shown that the NOTCH pathway is involved in the occurrence, development, and drug resistance of melanoma [54].

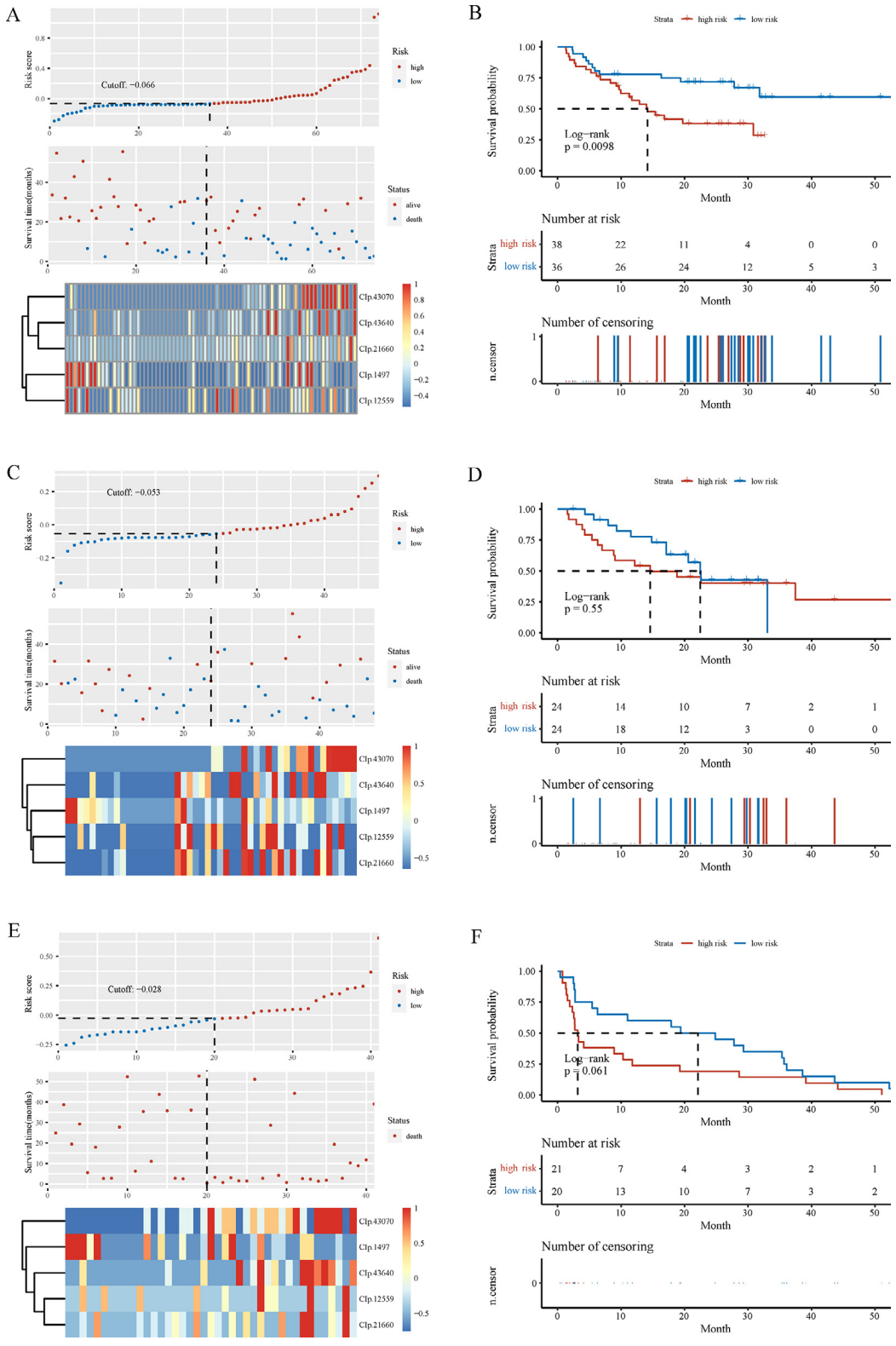

Fig. 3. Characteristics of the prognostic circRNAs signature and Kaplan-Meier estimates for PFS in the training and validation cohorts. A. Characteristics of the prognostic signature in the training cohort. top: the risk score of each patient in the training cohort; middle: PFS and survival status of patients in the training cohort; bottom: heat map of gene expression profiles of patients in the training cohort. B. PFS in the training cohort stratified by the prognostic signature into high and low-risk groups with the *P* value shown. C. Characteristics of the prognostic signature in the internal validation cohort. top: the risk score of each patient in the internal validation cohort; middle: PFS and survival status of patients in the internal validation cohort; bottom: heat map of gene expression profiles of patients in the internal validation cohort. D. PFS in the internal validation cohort stratified by the prognostic signature into high and low-risk groups with the *P* value shown. E. Characteristics of the prognostic signature in the external validation cohort. top: the risk score of each patient in the external validation cohort; middle: PFS and survival status of patients in the external validation cohort; bottom: heat map of gene expression profiles of patients in the external validation cohort. F. PFS in the external validation cohort stratified by the prognostic signature into high and low-risk groups with the *P* value shown. The black dotted line represents the prognostic signature cutoff dividing patients into high and low-risk groups, and the *P* value was calculated using the log-rank test.

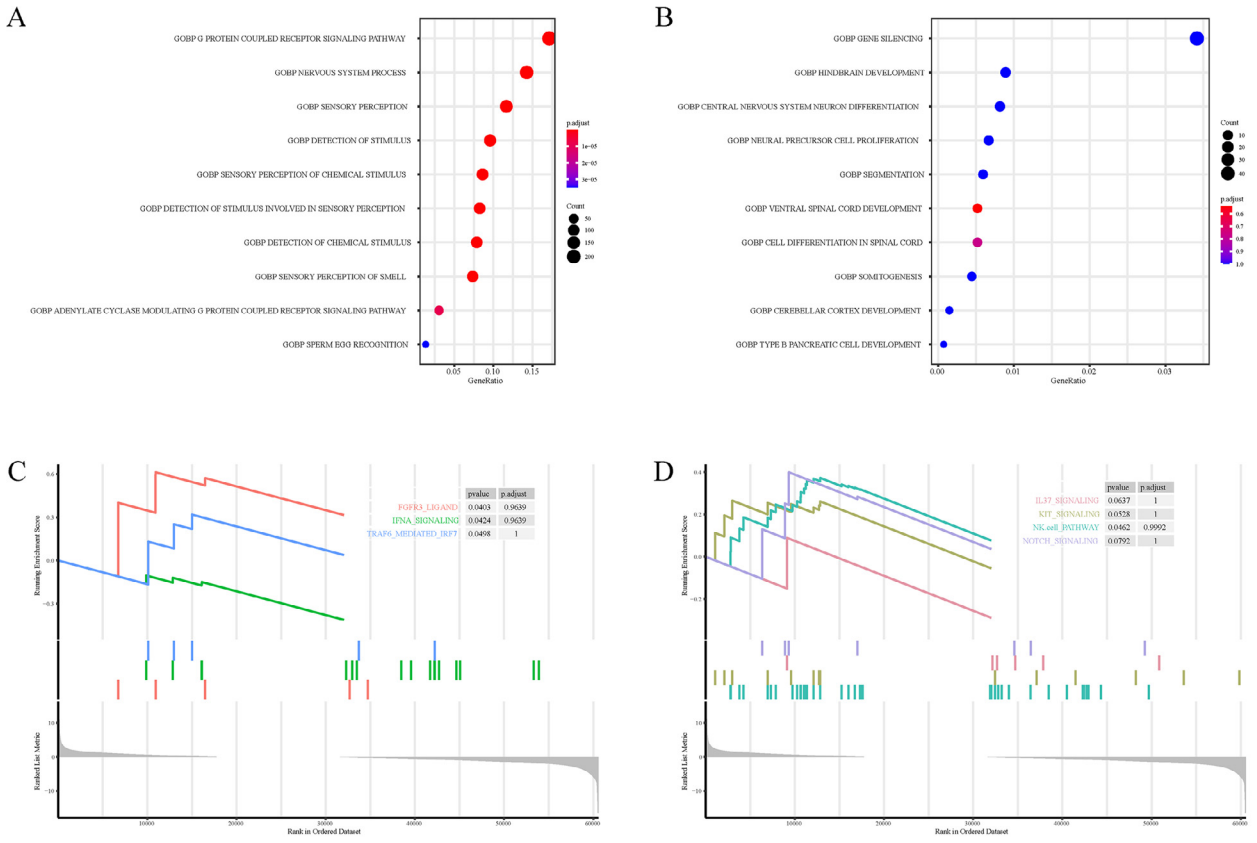

Fig. 4. Functional enrichment in the training and validation cohorts. A. Biological process of down-regulated genes in phs000452. B. Biological process of up-regulated genes in phs000452. C. GSEA of down-regulated genes in phs000452. D. GSEA of up-regulated genes in phs000452.

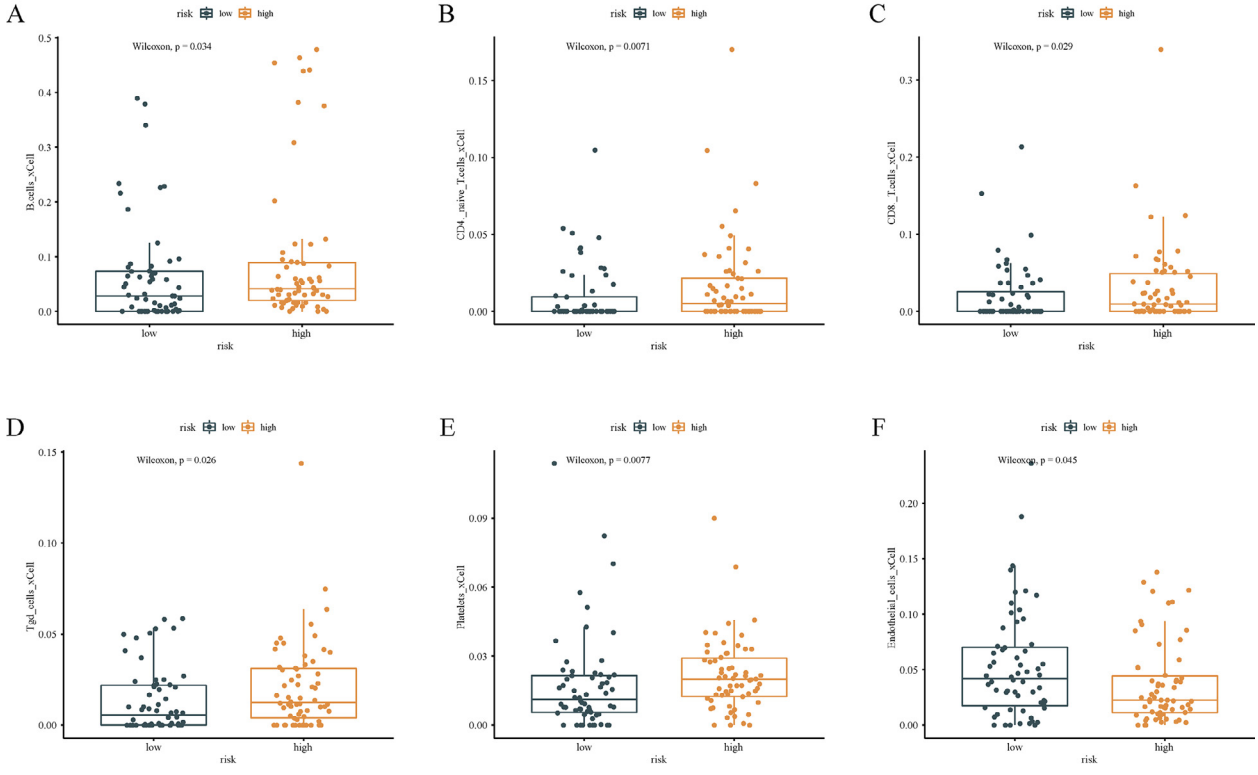

Fig. 5. Quantification of immune microenvironment. A. B cells. B. $CD4^+$ naïve T cells. C. $CD8^+$ T cells. D. $\gamma\delta$ T cells. E. Platelets. F. Endothelial cells. Wilcoxon test was conducted.

All these known information reflect the reliability of the signature we established in the present study from the side.

It should be noted that until today no direct evidence, based on clinical or basic research, exists that circRNAs could be considered as biomarkers in PD-1 treatment. However, studies already demonstrated that circRNAs affect the tumor microenvironment and thereby impact the PD-1 treatment. We stress that in the future validation experiments through *in vivo* or *in vitro* experiments are necessary. Furthermore, validation studies of prospective nature with melanoma patients have to be initiated.

To summarize, certain limitations in our study need to be acknowledged. First, the prognostic circRNAs signature we obtained here may provide new ideas and insights for predicting the survival benefit of melanoma patients receiving anti-PD-1 monotherapy. However, we cannot get all clinicopathological characteristics for each patient since all data are from public database. Second, we only conducted functional analysis and immune cell abundance in phs000452 due to the relatively small sample size of PRJEB23709; more in vivo or in vitro experiments are needed to further elucidate the underlying biological mechanisms. In addition, only pre-treatment tumor biopsies data from advanced melanoma patients treated with anti-PD-1 monotherapy was included in this study, anti-PD-1 monotherapy (nivolumab or pembrolizumab) in phs000452 and PRJEB23709 is not exactly consistent. Finally, this is a retrospective study, more multicenter, prospective, and large-scale studies are warranted to test our findings before the prognostic circRNAs signature is applied clinically.

Conclusions

Overall, we identified a prognostic circRNAs signature to reflect the different OS and PFS among advanced melanoma patients who are receiving anti-PD-1 monotherapy, which may be helpful for the risk stratification of these patients. Our findings also provide hints that immune response and currently known pathways related to tumor immune microenvironment are related to the prognosis. The prognostic circRNAs signature could therefore be a novel independent prognostic predictor and immunotherapy marker for filtering advanced melanoma patients who may benefit from anti-PD-1 monotherapy. These results offer novel insights into the prognosis evaluation of advanced melanoma and provide a reference for future studies on anti-PD-1 monotherapy in advanced melanoma.

Data availability

Raw sequencing data are available in dbGaP (Melanoma Genome Sequencing Project, accession number phs000452.v.3.p1, https://www.ncbi.nlm.nih.gov/projects/gap/cgi-bin/study.cgi?study_id=phs000452.v3.p1) and EMBL-EBI (RNA sequencing of immunotherapy patients in metastatic melanoma, accession number PRJEB23709, https://www.ebi.ac.uk/ena/browser/view/PRJEB23709).

Authors' contribution

All authors have read and agreed to the published version of the manuscript.

Funding

This research was funded by the National Natural Science Foundation of China (Grant No. 81660512), the Natural Science Foundation of Guizhou Province (Grant No. ZK2021-YB435), Scientific Research Project of the Education Department of Guizhou Province (Grant No. QJJ2022-224), Research Programs of Health Commission Foundation of Guizhou Province (Grant Nos. gzwjkj2023-1-042), Lian Yun Gang Shi Hui Lan Public Foundation (Grant No. HL-HS2020-92), Collaborative Innovation Center of Chinese Ministry of Education (Grant Number:2020-39).

CRediT authorship contribution statement

Jian-Guo Zhou: Conceptualization, Methodology, Validation, Data curation, Writing – original draft, Supervision, Project administration, Funding acquisition. **Rui Liang:** Writing – original draft, Writing – review & editing, Visualization. **Hai-Tao Wang:** Methodology, Visualization. **Su-Han Jin:** Conceptualization. **Wei Hu:** Data curation. **Benjamin Frey:** Writing – review & editing. **Rainer Fietkau:** Validation. **Markus Hecht:** Validation, Writing – review & editing. **Hu Ma:** Conceptualization, Validation, Data curation, Writing – review & editing, Supervision, Project administration, Funding acquisition. **Udo S. Gaipl:** Conceptualization, Validation, Data curation, Writing – review & editing, Supervision, Project administration.

Acknowledgments

We would like to thank Tuba N. Gide *et al.* who released and shared their data on the EMBL-EBI database (PRJEB23709). We also thank Levi Garraway, Eric Lander, and Stacey Gabriel, who submitted data from the original study to dbGaP (phs000452.v.3.p1). The present work was performed by Jian-Guo Zhou in (partial) fulfilment of the requirements for containing the degree "Dr. rer. biol. hum".

Supplementary materials

Supplementary material associated with this article can be found, in the online version, at doi:10.1016/j.neo.2023.100877.

References

[1] RN Amaria, SM Reddy, HA Tawbi, MA Davies, MI Ross, IC Glitza, JN Cormier, C Lewis, W-J Hwu, E Hanna, et al., Neoadjuvant immune checkpoint blockade in high-risk resectable melanoma, Nat. Med. 24 (2018) 1649–1654.
[2] C Robert, J Schachter, GV Long, A Arance, JJ Grob, L Mortier, A Daud, MS Carlino, C McNeil, M Lotem, et al., Pembrolizumab versus ipilimumab in advanced melanoma, N. Engl. J. Med. 372 (2015) 2521–2532.
[3] PA Ascierto, M Del Vecchio, M Mandalá, H Gogas, AM Arance, S Dalle, CL Cowey, M Schenker, J-J Grob, V Chiarion-Sileni, et al., Adjuvant nivolumab versus ipilimumab in resected stage IIIB-C and stage IV melanoma (CheckMate 238): 4-year results from a multicentre, double-blind, randomised, controlled, phase 3 trial, Lancet Oncol. 21 (2020) 1465–1477.
[4] T André, K-K Shiu, TW Kim, BV Jensen, LH Jensen, C Punt, D Smith, R Garcia–Carbonero, M Benavides, P Gibbs, et al., Pembrolizumab in microsatellite-instability-high advanced colorectal cancer, N. Engl. J. Med. 383 (2020) 2207–2218.
[5] MJ Overman, R McDermott, JL Leach, S Lonardi, H-J Lenz, MA Morse, J Desai, A Hill, M Axelson, RA Moss, et al., Nivolumab in patients with metastatic DNA mismatch repair-deficient or microsatellite instability-high colorectal cancer (CheckMate 142): an open-label, multicentre, phase 2 study, Lancet Oncol. 18 (2017) 1182–1191.
[6] MD Hellmann, L Paz-Ares, R Bernabe Caro, B Zurawski, S-W Kim, E Carcereny Costa, K Park, A Alexandru, L Lupinacci, E de la Mora Jimenez, et al., Nivolumab plus ipilimumab in advanced non-small-cell lung cancer, N. Engl. J. Med. 381 (2019) 2020–2031.
[7] H Borghaei, L Paz-Ares, L Horn, DR Spigel, M Steins, NE Ready, LQ Chow, EE Vokes, E Felip, E Holgado, et al., Nivolumab versus docetaxel in advanced nonsquamous non-small-cell lung cancer, N. Engl. J. Med. 373 (2015) 1627–1639.
[8] S Bagchi, R Yuan, EG Engleman, Immune checkpoint inhibitors for the treatment of cancer: clinical impact and mechanisms of response and resistance, Annu Rev Pathol 16 (2021) 223–249.
[9] A Snyder, V Makarov, T Merghoub, J Yuan, JM Zaretsky, A Desrichard, LA Walsh, MA Postow, P Wong, TS Ho, et al., Genetic basis for clinical response to CTLA-4 blockade in melanoma, N. Engl. J. Med. 371 (2014) 2189–2199.
[10] R Cristescu, R Mogg, M Ayers, A Albright, E Murphy, J Yearley, X Sher, XQ Liu, H Lu, M Nebozhyn, et al., Pan-tumor genomic biomarkers for PD-1 checkpoint blockade-based immunotherapy, Science 362 (2018) eaar3593.
[11] Y Wang, H Zhang, C Liu, Z Wang, W Wu, N Zhang, L Zhang, J Hu, P Luo, J Zhang, et al., Immune checkpoint modulators in cancer immunotherapy: recent advances and emerging concepts, J. Hematol. Oncol. 15 (2022) 111.
[12] S Nisar, AA Bhat, M Singh, T Karedath, A Rizwan, S Hashem, P Bagga, R Reddy, F Jamal, S Uddin, et al., Insights into the role of CircRNAs: biogenesis, characterization, functional, and clinical impact in human malignancies, Front. Cell Dev. Biol. 9 (2021) 617281.
[13] X Gao, X Xia, F Li, M Zhang, H Zhou, X Wu, J Zhong, Z Zhao, K Zhao, D Liu, et al., Circular RNA-encoded oncogenic E-cadherin variant promotes glioblastoma tumorigenicity through activation of EGFR-STAT3 signalling, Nat. Cell Biol. 23 (2021) 278–291.
[14] L Qian, S Yu, Z Chen, Z Meng, S Huang, P Wang, The emerging role of circRNAs and their clinical significance in human cancers, Biochim. Biophys. Acta Rev. Cancer 1870 (2018) 247–260.

[15] Y Pan, KE Kadash-Edmondson, R Wang, J Phillips, S Liu, A Ribas, R Aplenc, ON Witte, Y Xing, RNA dysregulation: an expanding source of cancer immunotherapy targets, Trend. Pharmacol. Sci. 42 (2021) 268–282.
[16] LS Kristensen, MS Andersen, LVW Stagsted, KK Ebbesen, TB Hansen, J Kjems, The biogenesis, biology and characterization of circular RNAs, Nat. Rev. Genet. 20 (2019) 675–691.
[17] Vo JN, Cieslik M, Zhang Y, Shukla S, Xiao L, Zhang Y, Wu Y-M, Dhanasekaran SM, Engelke CG, Cao X, et al. (2019). The landscape of circular RNA in cancer cell 176, 869-881.
[18] S Chen, V Huang, X Xu, J Livingstone, F Soares, J Jeon, Y Zeng, JT Hua, J Petricca, H Guo, et al., Widespread and functional RNA circularization in localized prostate cancer, Cell 176 (2019) 831–843.
[19] D Liu, B Schilling, D Liu, A Sucker, E Livingstone, L Jerby-Arnon, L Zimmer, R Gutzmer, I Satzger, C Loquai, et al., Integrative molecular and clinical modeling of clinical outcomes to PD1 blockade in patients with metastatic melanoma, Nat. Med. 25 (2019) 1916–1927.
[20] TN Gide, C Quek, AM Menzies, AT Tasker, P Shang, J Holst, J Madore, SY Lim, R Velickovic, M Wongchenko, et al., Distinct immune cell populations define response to anti-PD-1 monotherapy and anti-PD-1/anti-CTLA-4 combined therapy, Cancer Cell 35 (2019) 238–255.
[21] F Madeira, YM Park, J Lee, N Buso, T Gur, N Madhusoodanan, P Basutkar, ARN Tivey, SC Potter, RD Finn, et al., The EMBL-EBI search and sequence analysis tools APIs in 2019, Nucleic. Acids. Res. 47 (2019) W636–W641.
[22] A Dobin, CA Davis, F Schlesinger, J Drenkow, C Zaleski, S Jha, P Batut, M Chaisson, TR Gingeras, STAR: ultrafast universal RNA-seq aligner, Bioinformatics 29 (2013) 15–21.
[23] Y Liao, GK Smyth, W Shi, featureCounts: an efficient general purpose program for assigning sequence reads to genomic features, Bioinformatics 30 (2013) 923–930.
[24] J-G Zhou, B Liang, J-G Liu, S-H Jin, S-S He, B Frey, N Gu, R Fietkau, M Hecht, H Ma, et al., Identification of 15 lncRNAs signature for predicting survival benefit of advanced melanoma patients treated with anti-PD-1 monotherapy, Cells 10 (2021) 977.
[25] T Jakobi, C Dieterich, Computational approaches for circular RNA analysis, Wiley Interdiscip. Rev. RNA 10 (2019) e1528.
[26] T-J Chuang, C-S Wu, C-Y Chen, L-Y Hung, T-W Chiang, M-Y Yang, NCLscan: accurate identification of non-co-linear transcripts (fusion, trans-splicing and circular RNA) with a good balance between sensitivity and precision, Nucleic. Acid. Res. 44 (2016) e29.
[27] X-O Zhang, R Dong, Y Zhang, J-L Zhang, Z Luo, J Zhang, L-L Chen, L Yang, Diverse alternative back-splicing and alternative splicing landscape of circular RNAs, Genome Res. 26 (2016) 1277–1287.
[28] S Aufiero, YJ Reckman, AJ Tijsen, YM Pinto, EE Creemers, circRNAprofiler: an R-based computational framework for the downstream analysis of circular RNAs, BMC Bioinf. 21 (2020) 164.
[29] AJ McEligot, V Poynor, R Sharma, A Panangadan, Logistic LASSO regression for dietary intakes and breast cancer, Nutrients 12 (2020) 2652.
[30] R Dong, X-K Ma, G-W Li, L Yang, CIRCpedia v2: an updated database for comprehensive circular RNA annotation and expression comparison, Genom. Proteom. Bioinformat. 16 (2018) 226–233.
[31] J-G Zhou, B Liang, S-H Jin, H-L Liao, G-B Du, L Cheng, H Ma, US Gaipl, Development and validation of an RNA-Seq-based prognostic signature in neuroblastoma, Front. Oncol. 9 (2019) 1361.
[32] PJ Heagerty, T Lumley, MS Pepe, Time-dependent ROC curves for censored survival data and a diagnostic marker, Biometrics 56 (2000) 337–344.
[33] W-C Lu, H Chen, B Liang, C-P Ou, M Zhang, Q Yue, J Xie, Integrative analyses and verification of the expression and prognostic significance for RCN1 in glioblastoma multiforme, Front. Mol. Biosci. 8 (2021) 736947.
[34] B Liang, Y Liang, R Li, H Zhang, N Gu, Integrating systematic pharmacology-based strategy and experimental validation to explore the synergistic pharmacological mechanisms of Guanxin V in treating ventricular remodeling, Bioorg. Chem. 115 (2021) 105187.
[35] R-H Yang, B Liang, J-H Li, X-B Pi, K Yu, S-J Xiang, N Gu, X-D Chen, S-T Zhou, Identification of a novel tumour microenvironment-based prognostic biomarker in skin cutaneous melanoma, J. Cell. Mol. Med. 25 (2021) 10990–11001.
[36] D Zeng, Z Ye, R Shen, G Yu, J Wu, Y Xiong, R Zhou, W Qiu, N Huang, L Sun, et al., IOBR: multi-omics immuno-oncology biological research to decode tumor microenvironment and signatures, Front. Immunol. 12 (2021) 687975.
[37] D Aran, Z Hu, AJ Butte, xCell: digitally portraying the tissue cellular heterogeneity landscape, Genome Biol. 18 (2017) 220.
[38] EA Eisenhauer, P Therasse, J Bogaerts, LH Schwartz, D Sargent, R Ford, J Dancey, S Arbuck, S Gwyther, M Mooney, et al., New response evaluation criteria in solid tumours: revised RECIST guideline (version 1.1), Eur. J. Cancer 45 (2009) 228–247.
[39] Y Wang, M Mashock, Z Tong, X Mu, H Chen, X Zhou, H Zhang, G Zhao, B Liu, X Li, Changing technologies of RNA sequencing and their applications in clinical oncology, Front. Oncol. 10 (2020) 447.
[40] L Li, S Khan, S Li, S Wang, F Wang, Noncoding RNAs: emerging players in skin cancers pathogenesis, Am. J. Cancer Res. 11 (2021) 5591–5608.
[41] J Chen, X Zhou, J Yang, Q Sun, Y Liu, N Li, Z Zhang, H Xu, Circ-GLI1 promotes metastasis in melanoma through interacting with p70S6K2 to activate Hedgehog/GLI1 and Wnt/β-catenin pathways and upregulate Cyr61, Cell Death. Dis. 11 (2020) 596.
[42] C-Y Wei, M-X Zhu, N-H Lu, J-Q Liu, Y-W Yang, Y Zhang, Y-D Shi, Z-H Feng, J-X Li, F-Z Qi, et al., Circular RNA circ_0020710 drives tumor progression and immune evasion by regulating the miR-370-3p/CXCL12 axis in melanoma, Mol. Cancer 19 (2020) 84.
[43] CA Natale, J Li, J Zhang, A Dahal, T Dentchev, BZ Stanger, TW Ridky, Activation of G protein-coupled estrogen receptor signaling inhibits melanoma and improves response to immune checkpoint blockade, eLife 7 (2018) e31770.
[44] MW Millar, N Corson, L Xu, The adhesion G-protein-coupled receptor, GPR56/ADGRG1, inhibits cell-extracellular matrix signaling to prevent metastatic melanoma growth, Front. Oncol. 8 (2018) 8.
[45] K Tworkoski, G Singhal, S Szpakowski, CI Zito, A Bacchiocchi, V Muthusamy, M Bosenberg, M Krauthammer, R Halaban, DF Stern, Phosphoproteomic screen identifies potential therapeutic targets in melanoma, Mol. Cancer Res. 9 (2011) 801–812.
[46] L Li, S Zhang, H Li, H Chou, FGFR3 promotes the growth and malignancy of melanoma by influencing EMT and the phosphorylation of ERK, AKT, and EGFR, BMC Cancer 19 (2019) 963.
[47] V Yadav, X Zhang, J Liu, S Estrem, S Li, X-Q Gong, S Buchanan, JR Henry, JJ Starling, S-B Peng, Reactivation of mitogen-activated protein kinase (MAPK) pathway by FGF receptor 3 (FGFR3)/Ras mediates resistance to vemurafenib in human B-RAF V600E mutant melanoma, J. Biol. Chem. 287 (2012) 28087–28098.
[48] A Thiem, S Hesbacher, H Kneitz, T di Primio, MV Heppt, HM Hermanns, M Goebeler, S Meierjohann, R Houben, D Schrama, IFN-gamma-induced PD-L1 expression in melanoma depends on p53 expression, J. Exp. Clin. Cancer Res. 38 (2019) 397.
[49] CS Grasso, J Tsoi, M Onyshchenko, G Abril-Rodriguez, P Ross-Macdonald, M Wind-Rotolo, A Champhekar, E Medina, DY Torrejon, DS Shin, et al., Conserved interferon-γ signaling drives clinical response to immune checkpoint blockade therapy in Melanoma, Cancer Cell 38 (2020) 500–515 e503.
[50] DG Osborne, J Domenico, Y Luo, AL Reid, C Amato, Z Zhai, D Gao, M Ziman, CA Dinarello, WA Robinson, et al., Interleukin-37 is highly expressed in regulatory T cells of melanoma patients and enhanced by melanoma cell secretome, Mol. Carcinog. 58 (2019) 1670–1679.
[51] D Schadendorf, DE Fisher, C Garbe, JE Gershenwald, J-J Grob, A Halpern, M Herlyn, MA Marchetti, G McArthur, A Ribas, et al., Melanoma, Nat. Rev. Dis. Primers 1 (2015) 15003.
[52] L Zhu, S Kalimuthu, P Gangadaran, JM Oh, HW Lee, SH Baek, SY Jeong, S-W Lee, J Lee, B-C Ahn, Exosomes derived from natural killer cells exert therapeutic effect in Melanoma, Theranostics 7 (2017) 2732–2745.
[53] 0000-0001-9019-1426 O T Nakamura, T Sato, R Endo, S Sasaki, N Takahashi, Y Sato, M Hyodo, Y Hayakawa, H Harashima, STING agonist loaded lipid nanoparticles overcome anti-PD-1 resistance in melanoma lung metastasis via NK cell activation, J. Immunother. Cancer 9 (2021) e002852.
[54] X Gao, G Chen, H Cai, X Wang, K Song, L Liu, T Qiu, Y He, Aberrantly enhanced melanoma-associated antigen (MAGE)-A3 expression facilitates cervical cancer cell proliferation and metastasis via actuating Wnt signaling pathway, Biomed. Pharmacother. 122 (2020) 109710.